

Hole-Doped Room-Temperature Superconductivity in $\text{H}_3\text{S}_{1-x}\text{Z}_x$ ($\text{Z}=\text{C}, \text{Si}$)

Yanfeng Ge,^{1,2} Fan Zhang,^{3,*} Ranga P. Dias,^{4,5} Russell J. Hemley,^{6,7} and Yugui Yao^{2,†}

¹State Key Laboratory of Metastable Materials Science and Technology and
Key Laboratory for Microstructural Materials Physics of Hebei Province,
School of Science, Yanshan University, Qinhuangdao, 066004, China

²Key Laboratory of Advanced Optoelectronic Quantum Architecture and Measurement,
Ministry of Education, School of Physics, Beijing Institute of Technology, Beijing 100081, China

³Department of Physics, University of Texas at Dallas, Richardson, Texas 75080, USA

⁴Department of Mechanical Engineering, University of Rochester, Rochester, New York 14627, USA

⁵Department of Physics and Astronomy, University of Rochester, Rochester, New York 14627, USA

⁶Department of Physics, University of Illinois at Chicago, Chicago, Illinois 60607, USA

⁷Department of Chemistry, University of Illinois at Chicago, Chicago, Illinois 60607, USA

(Dated: February 2, 2022)

We examine the effects of the low-level substitution of S atoms by C and Si atoms on the superconductivity of H_3S with the $Im\bar{3}m$ structure at megabar pressures. The hole doping can fine-tune the Fermi energy to reach the electronic density-of-states peak maximizing the electron-phonon coupling. This can boost the critical temperature from the original 203 K to 289 K and 283 K, respectively, for $\text{H}_3\text{S}_{0.962}\text{C}_{0.038}$ at 260 GPa and $\text{H}_3\text{S}_{0.960}\text{Si}_{0.040}$ at 230 GPa. The former may provide an explanation for the recent experimental observation of room-temperature superconductivity in a highly compressed C-S-H system [Nature **586**, 373-377 (2020)]. Our work opens a new avenue for substantially raising the critical temperatures of hydrogen-rich materials.

Pursuing room-temperature superconductors has been a major theme in condensed-matter and materials physics since the discovery of superconductivity in 1911. According to the Bardeen–Cooper–Schrieffer (BCS) theory, strong electron-phonon coupling and high phonon frequencies can conspire to produce superconductivity exhibiting high critical temperatures (T_c 's). These two conditions can be achieved via strong covalent metallicity and low atomic mass, respectively. Naturally, metallic hydrogen and hydrogen-rich materials in general under pressure are plausible candidate high- T_c superconductors [1–10]. As a prime example, hydrogen sulfide H_3S with the $Im\bar{3}m$ structure has been theoretically predicted [11, 12] and experimentally confirmed [13, 14] to exhibit a maximum T_c of 203 K at 150 GPa. Though a range of T_c 's has been reported in various studies [13–18], the maximum T_c of at least 180 K for H_3S has now been reproduced in several different experiments [13, 14, 17]. This breakthrough has attracted a great deal of research interest [19–24]. In particular, it has been predicted that under hole doping the T_c of $\text{H}_3\text{S}_{0.927}\text{P}_{0.075}$ can be as high as 280 K at 250 GPa [25]. To date a variety of new hydrogen-rich materials with different structures have been proposed based on first-principles calculations [26–31]. As a paradigmatic system, the lanthanum superhydride LaH_{10} with its novel hydrogen clathrate structure has been experimentally demonstrated to exhibit T_c 's of 250–260 K at pressures of 170–185 GPa [32–34].

A very recent experimental study has reported superconductivity in the C-S-H system at pressures of 140–275 GPa, with the highest T_c of 288 K at 267 GPa demonstrating room-temperature superconductivity [35]. Since the underlying crystal structure has yet to be determined, pressure-induced structural changes over the measured range cannot be ruled out. However, the current experimental data are consistent with a continuous increase in T_c with pressure but perhaps a discontinuous dT_c/dP near 230 GPa, suggesting a gradual

structural deformation instead of an abrupt structural transition near that pressure. More experimental data are obviously required to establish the trend of T_c versus pressure, and more importantly chemical analysis and X-ray diffraction are required to reveal the composition and crystal structure of the superconducting component in the C-S-H system.

Interestingly, the room-temperature superconductivity in the C-S-H system and its T_c pressure dependence beginning below 200 GPa [35] are strongly reminiscent of the predicted pressure effect on T_c of hole-doped $\text{H}_3\text{S}_{1-x}\text{P}_x$ and $\text{H}_3\text{S}_{1-x}\text{Si}_x$ [25]. Here we systematically study the effects of C and Si substitution for S on the superconductivity of H_3S with the cubic $Im\bar{3}m$ structure at megabar pressures based on first-principles calculations with the virtual crystal approximation (VCA) [25]. The cubic structure is examined here since it gives the highest T_c for H_3S [14]; the effects of substitution on phases derived from lower symmetry structures [11, 30, 31, 36–40] will be studied in future work. As demonstrated previously [25] and below, low-level substitution can fine-tune the Fermi energy to reach the electronic density-of-states (DOS) peak and thus maximize the electron-phonon coupling. It turns out that this can boost the T_c from the original 203 K to 289 K and 283 K, respectively, for $\text{H}_3\text{S}_{0.962}\text{C}_{0.038}$ at 260 GPa and $\text{H}_3\text{S}_{0.960}\text{Si}_{0.040}$ at 230 GPa. The former may provide an explanation for the recent experimental observation of room-temperature superconductivity in the C-S-H system including its overall T_c pressure dependence [35]. The results thus also suggest an effect of C incorporation below 200 GPa.

Following the approach introduced in Ref. 25, our calculations were performed within the framework of ABINIT [41–44] using the local-density approximation. The ion and electron interactions were treated with Hartwigsen-Goedecker-Hutter pseudopotentials [45]. The electronic ground-state properties were calculated on a $32 \times 32 \times 32$ Monkhorst-

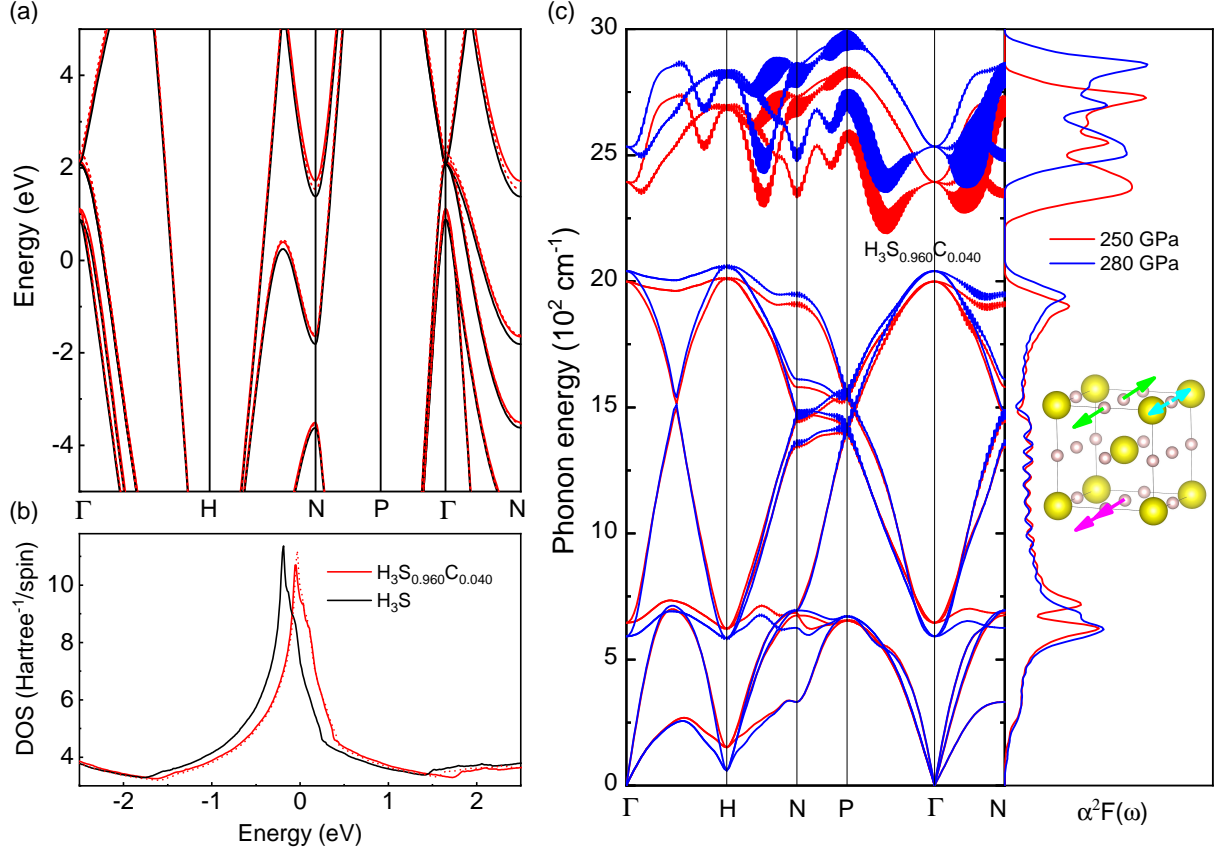


FIG. 1. (a) Band structures and (b) DOS of H₃S at 220 GPa (black), H₃S_{0.960}C_{0.040} at 220 GPa (solid red), and H₃S_{0.960}C_{0.040} at 240 GPa (dashed red), with their Fermi energies set to be zero. (c) Phonon dispersion and Eliashberg function $\alpha^2F(\omega)$ of H₃S_{0.960}C_{0.040} at 250 GPa (red) and 280 GPa (blue). The magnitudes of phonon linewidths are indicated by the line thickness. Inset: the low-frequency (magenta) and high-frequency (green) H-S bond-bending modes around 600 (2000) cm⁻¹ and the H-S bond-stretching modes around 2500 cm⁻¹ (cyan).

Pack k -mesh using the kinetic energy cutoff of 800 eV. The phonon dispersions and the electron-phonon couplings were calculated on an $8 \times 8 \times 8$ q -grid using the density functional perturbation theory [46]. The atomic substitution was simulated by the self-consistent VCA, where the virtual pseudopotentials of $S_{1-x}Z_x$ were set to be $V_{VCA} = (1-x)V_S + xV_Z$.

The superconductivity of H₃S can be accurately described by the BCS theory, which underlines the aforementioned strong electron-phonon coupling and high phonon frequencies as the two most important factors in producing the high T_c in this class of materials. Here we focus on the former factor, or equivalently the effect of the electronic DOS, for reasons that becomes clear below. H₃S has a DOS that reaches 7.43 Hartree⁻¹/spin at its Fermi level [21], because of the presence of a van Hove singularity in the vicinity, as shown in Fig. 1. By substituting the S atoms with C and Si, the H₃S system can be hole doped, and the Fermi level can be moved closer to the DOS peak, and by increasing the pressure, the DOS peak can be further enhanced. Both effects are illustrated in Fig. 1(b). The dynamical stability of the crystal structure limits the substitution level to $x \leq 0.050$ for H₃S_{1-x}Z_x (Z=C, Si) hereafter.

Figure 1(c) compares the phonon dispersions of H₃S_{0.960}C_{0.040} at 250 and 280 GPa. The coupling of Fermi-level electrons with specific phonons is indicated by the thickness of the dispersion curves, i.e., the magnitudes of phonon linewidths

$$\gamma_{q\nu} = 2\pi\omega_{q\nu} \sum_{ij\mathbf{k}} |M_{i\mathbf{k},j\mathbf{k}+\mathbf{q}}^\nu|^2 \delta(\epsilon_{i\mathbf{k}} - \epsilon_F) \delta(\epsilon_{j\mathbf{k}+\mathbf{q}} - \epsilon_F), \quad (1)$$

where $M_{i\mathbf{k},j\mathbf{k}+\mathbf{q}}^\nu$ are the microscopic electron-phonon matrix elements. High-frequency H-S (or H-Z) bond-stretching modes near 2500 cm⁻¹ have the largest phonon linewidths, indicating strong electron-phonon coupling of the H-based vibrations. One such high-frequency phonon mode and two lower-frequency modes are illustrated in the inset of Fig. 1(c).

The superconductivity of H₃S_{1-x}Z_x (Z=C, Si) can be estimated by Eliashberg theory [47], which takes into account the renormalization of electron-electron repulsion by electron-phonon interactions. This celebrated theory has been successfully used in predictions of superconductivity in hydrogen-rich materials as well as ambient-pressure conventional superconductors. Figure 2(a) shows that for both C- and Si-substitutions at 250 GPa the DOS at the Fermi level increases

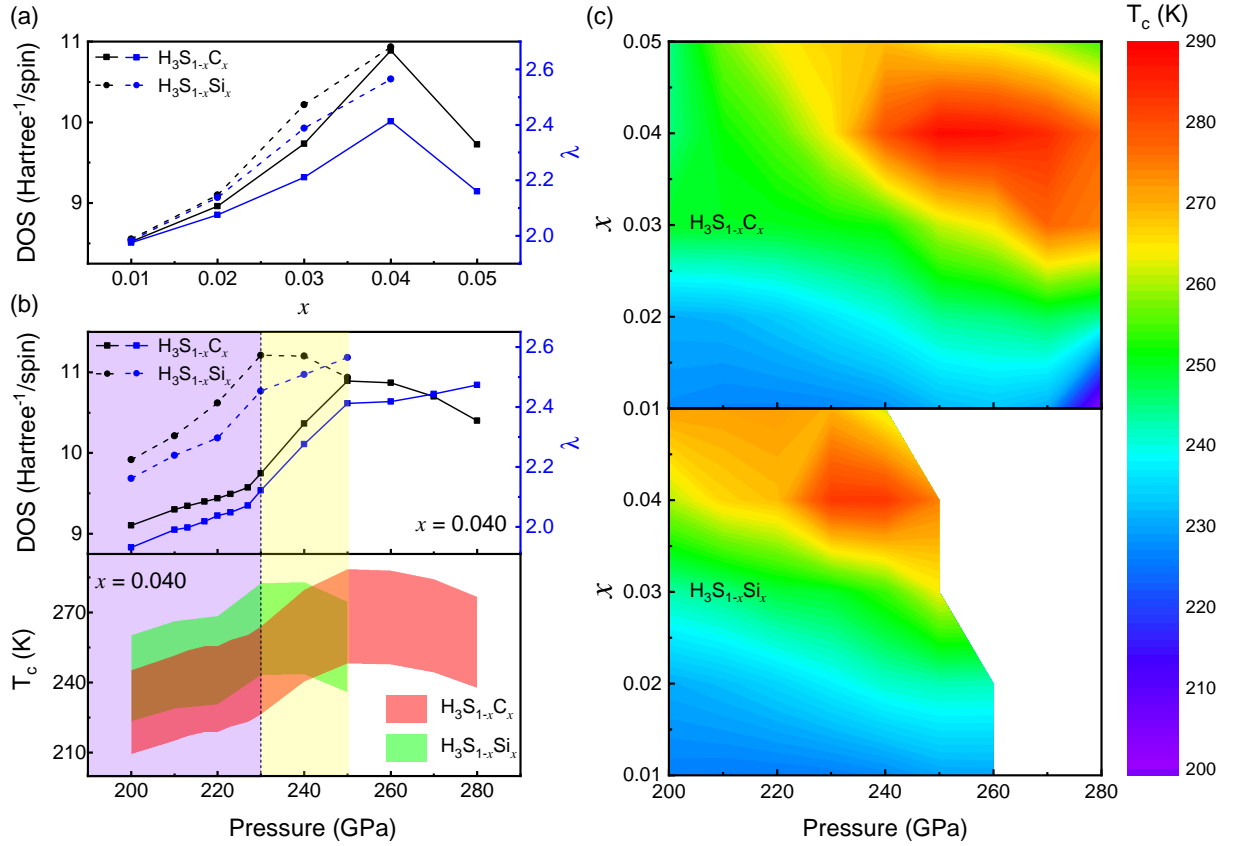


FIG. 2. (a) DOS (black) and electron-phonon coupling λ (blue) of cubic $\text{H}_3\text{S}_{1-x}\text{Z}_x$ ($\text{Z}=\text{C}, \text{Si}$) versus x at 250 GPa. Solid and dashed lines denote the results for $\text{H}_3\text{S}_{1-x}\text{C}_x$ (square) and $\text{H}_3\text{S}_{1-x}\text{Si}_x$ (circle), respectively. (b) DOS (black), λ (blue), and T_c (shaded) versus pressure at $x = 0.040$. For each T_c curve, the upper and lower bounds are obtained by choosing $\mu^* = 0.10$ and 0.15 , respectively. (c) The T_c maps of $\text{H}_3\text{S}_{1-x}\text{C}_x$ and $\text{H}_3\text{S}_{1-x}\text{Si}_x$ versus substitution level and pressure for $\mu^* = 0.10$. At high pressures or high substitution levels, cubic $\text{H}_3\text{S}_{1-x}\text{Si}_x$ becomes unstable; thus no data are shown.

with increasing the substitution level x , reaches a maximum around $x = 0.040$, and then starts to decrease. This trend is similar to that found for $\text{H}_3\text{S}_{1-x}\text{P}_x$ [25], and as anticipated C- or Si-substitution is almost twice as efficient as P-substitution for hole doping. For both cases, the electron-phonon coupling λ follows the trend of the DOS, as the influence of low substitution on the phonon frequency is weak and secondary. The upper-pressure limit of dynamical stability of cubic $Im\bar{3}m$ $\text{H}_3\text{S}_{1-x}\text{Z}_x$ varies with both Z and x . For example, the upper-pressure limit of $\text{H}_3\text{S}_{0.960}\text{C}_{0.040}$ is 280 GPa, and that of $\text{H}_3\text{S}_{0.960}\text{Si}_{0.040}$ is 250 GPa. Beyond these limits, acoustic phonons at the H point become imaginary signaling structural instabilities. As seen in Fig. 2(c), our study focuses on pressures of 200–280 GPa and the substitution levels up to $x = 0.050$. At these pressures $\text{H}_3\text{S}_{1-x}\text{C}_x$ is found to be dynamically stable, whereas $\text{H}_3\text{S}_{1-x}\text{Si}_x$ becomes unstable beyond about 250 GPa with a moderate x -dependence.

As shown in Fig. 2(b), for both C- and Si-substitutions at $x = 0.040$, the DOS at the Fermi level increases first and then decreases as the pressure increases. The maximum DOS occurs at different pressures for the two cases, i.e., 250 GPa for $\text{H}_3\text{S}_{0.960}\text{C}_{0.040}$ and 230 GPa for $\text{H}_3\text{S}_{0.960}\text{Si}_{0.040}$. Notably, for

C-substitution the DOS increases more markedly with pressure in the 230–250 GPa range than that at lower pressures. A possible reason is the complex influence of compression on the electronic structure around the Fermi level, as implied in Fig. 1(b) by the different DOS behavior at different pressures for a fixed doping level. By contrast, the λ 's in both cases increase monotonically with pressure. The different DOS and λ trends with pressure are likely due to softening of the phonons around 600 cm^{-1} . As marked by the magenta arrows in the inset of Fig. 1(c), these softened phonon modes, which also contribute to λ , are low-frequency H-S bond-bending modes [20]. As we see from $\lambda = 2 \int \omega^{-1} \alpha^2 F(\omega) d\omega$, the phonon softening is beneficial for enhancing λ . Indeed, there is a drop in the logarithmically averaged phonon frequency $\langle \omega \rangle_{\log}$ from 1364 K at 250 GPa to 1269 K at 280 GPa. This explains why λ exhibits a modest upward trend while the DOS decreases with increasing pressure.

Given the averaged phonon frequency $\langle \omega \rangle_{\log}$, effective Coulomb repulsion μ^* , and electron-phonon coupling λ , the Allen-Dynes-modified McMillan formula [48, 49]

$$T_c = f_1 f_2 \frac{\langle \omega \rangle_{\log}}{1.20} \exp \left[-\frac{1.04(1 + \lambda)}{\lambda - \mu^*(1 + 0.62\lambda)} \right] \quad (2)$$

can be implemented to predict the T_c . Here f_1 and f_2 are the strong coupling and shape correction factors [48], respectively; a reasonable range of μ^* is between 0.10 and 0.15 [50]. For H_3S at 200 GPa [13], our calculations yield the T_c of 194 K for $\mu^* = 0.12$ and 203 K for $\mu^* = 0.11$. Following the behavior of the DOS, the T_c increases faster in the 230–250 GPa range than that at lower pressures, as shown in Fig. 2(b). This behavior appears to parallel the upturn in T_c above 230 GPa observed experimentally in the C-S-H system [35]. While the DOS drops with increase in pressure as discussed above, the phonon softening enhances λ but weakens $\langle\omega\rangle_{\log}$. This implies a decrease of Debye temperature in the BCS theory. This suggests a maximum T_c versus pressure that tracks the behavior of the DOS. In order to display the joint influence of hole doping and high pressure, as well as to identify the maximum T_c , we plot the map of the T_c versus the substitution level and pressure for $\mu^* = 0.10$ in Fig. 2(c). In particular, the highest T_c are 289 K for $\text{H}_3\text{S}_{0.962}\text{C}_{0.038}$ at 260 GPa and 283 K for $\text{H}_3\text{S}_{0.960}\text{Si}_{0.040}$ at 230 GPa. The former is very close to the highest T_c of 288 K at 267 GPa observed in the C-S-H experiment [35]. Evidently in Fig. 2(c), the highest T_c 's are reached near the structural instabilities. This appears to be consistent with the picture that soft phonon modes can be important for T_c enhancement near structural instabilities in superconducting hydrides [51–53].

In conclusion, we have examined the effects of hole doping on the superconductivity of H_3S with the $Im\bar{3}m$ structure at megabar pressures by using the first-principles calculations with the VCA. This fine-tunes the Fermi energy to reach the peak in the electronic DOS, maximizes the electron-phonon coupling, and boosts the T_c to 289 K and 283 K, respectively, for $\text{H}_3\text{S}_{0.962}\text{C}_{0.038}$ at 260 GPa and $\text{H}_3\text{S}_{0.960}\text{Si}_{0.040}$ at 230 GPa. Because of the fewer valence electrons and the lighter atomic masses, the C- and Si-substitutions are more efficient in raising T_c than substitution by P [25]. Although less stable at the higher pressure, Si-substitution raises the T_c more than substitution by C below 240 GPa. Most importantly, the C-substitution may provide an explanation for the recent experimental observation of room-temperature superconductivity in the C-S-H system and its T_c pressure dependence above 200 GPa [35]. Our findings indicate that hole doping in general—not limited to C-, Si-, and P-substitutions—is a robust approach to maximize the T_c of H_3S . Looking forward, our study, together with Ref. 25, opens a new avenue for substantially raising the already high T_c 's of hydrogen-rich materials and calls for experimental investigation to systematically optimize the doping of these materials under pressure to reach still higher T_c 's.

We are grateful to Roald Hoffmann and Eva Zurek for valuable comments on this work. F.Z. is grateful to Anvar Zakhidov, Bing Lv, and Mikhail Erements for valuable discussions at the initial stage of this work. The work is supported by the National Key R&D Program of China (Grant No. 2020YFA0308800), the National Natural Science Foundation of China (Grants Nos. 11904312 and 11734003), the Strategic Priority Research Program of Chinese Academy of Sci-

ences (Grant No. XDB30000000), the Project of Hebei Educational Department (Grants No. QN2018012), the UT Dallas Research Enhancement Fund, the US National Science Foundation (Grant Nos. DMR-1933622 and DMR-1809649), and the US Department of Energy (Grant Nos. DE-SC0020340 and DE-NA0003975).

* zhang@utdallas.edu

† ygyao@bit.edu.cn

- [1] N. W. Ashcroft, Phys. Rev. Lett. **21**, 1748 (1968).
- [2] N. W. Ashcroft, Phys. Rev. Lett. **92**, 187002 (2004).
- [3] J. Feng, W. Grochala, T. Jaron, R. Hoffmann, A. Bergara, and N. W. Ashcroft, Phys. Rev. Lett. **96**, 017006 (2006).
- [4] J. S. Tse, Y. Yao, and K. Tanaka, Phys. Rev. Lett. **98**, 117004 (2007).
- [5] M. I. Erements, I. A. Trojan, S. A. Medvedev, J. S. Tse, and Y. Yao, Science **319**, 1506 (2008).
- [6] X.-J. Chen, J.-L. Wang, V. V. Struzhkin, H.-K. Mao, R. J. Hemley, and H.-Q. Lin, Phys. Rev. Lett. **101**, 077002 (2008).
- [7] Y. W. Li, G. Y. Gao, Y. Xie, Y. Ma, T. Cui, and G. Zou, Proc. Natl. Acad. Sci. U.S.A. **107**, 15708 (2010).
- [8] G. Gao, A. R. Oganov, P. Li, Z. Li, H. Wang, T. Cui, Y. Ma, A. Bergara, A. O. Lyakhov, and T. Iitaka, Proc. Natl. Acad. Sci. U.S.A. **107**, 1317 (2010).
- [9] C.-S. Zha, Z. Liu, and R. J. Hemley, Phys. Rev. Lett. **108**, 146402 (2012).
- [10] H. Wang, S. T. John, K. Tanaka, T. Iitaka, and Y. Ma, Proc. Natl. Acad. Sci. U.S.A. **109**, 6463 (2012).
- [11] Y. Li, J. Hao, H. Liu, Y. Li, and Y. Ma, J. Chem. Phys. **140**, 174712 (2014).
- [12] D. Duan, X. Huang, F. Tian, D. Li, H. Yu, Y. Liu, Y. Ma, B. Liu, and T. Cui, Phys. Rev. B **91**, 180502(R) (2015).
- [13] A. P. Drozdov, M. I. Erements, and I. A. Trojan, arXiv:1412.0460; A. P. Drozdov, M. I. Erements, I. A. Trojan, V. Ksenofontov, and S. I. Shylin, Nature **525**, 73 (2015).
- [14] M. Einaga, M. Sakata, T. Ishikawa, K. Shimizu, M. I. Erements, A. P. Drozdov, I. A. Trojan, N. Hirao, and Y. Ohishi, Nat. Phys. **12**, 835 (2016).
- [15] I. Trojan, A. Gavriluk, R. Ruffer, A. Chumakov, A. Mironovich, I. Lyubutin, D. Perekalin, A. P. Drozdov, and M. I. Erements, Science **351**, 1303 (2016).
- [16] X. Huang, X. Wang, D. Duan, B. Sundqvist, X. Li, Y. Huang, H. Yu, F. Li, Q. Zhou, B. Liu, and T. Cui, Natl. Sci. Rev. **6**, 713 (2019).
- [17] K. Shimizu, J. Phys. Soc. Jpn. **89**, 051005 (2020).
- [18] H.-K. Mao, X.-J. Chen, Y. Ding, B. Li, and L. Wang, Rev. Mod. Phys. **90**, 015007 (2018).
- [19] N. Bernstein, C. S. Hellberg, M. D. Johannes, I. I. Mazin, and M. J. Mehl, Phys. Rev. B **91**, 060511(R) (2015).
- [20] I. Errea, M. Calandra, C. J. Pickard, J. Nelson, R. J. Needs, Y. Li, H. Liu, Y. Zhang, Y. Ma, and F. Mauri, Phys. Rev. Lett. **114**, 157004 (2015).
- [21] D. A. Papaconstantopoulos, B. M. Klein, M. J. Mehl, and W. E. Pickett, Phys. Rev. B **91**, 184511 (2015).
- [22] R. Akashi, M. Kawamura, S. Tsuneyuki, Y. Nomura, and R. Arita, Phys. Rev. B **91**, 224513 (2015).
- [23] E. J. Nicol, and J. P. Carbotte, Phys. Rev. B **91**, 220507(R) (2015).
- [24] C. Heil, and L. Boeri, Phys. Rev. B **92**, 060508(R) (2015).

- [25] Y. Ge, F. Zhang, and Y. Yao, *Phys. Rev. B* **93**, 224513 (2016).
- [26] F. Peng, Y. Sun, C. Pickard, R. Needs, Q. Wu, and Y. Ma, *Phys. Rev. Lett.* **119**, 107001 (2017).
- [27] H. Liu, I. I. Naumov, R. Hoffmann, N. W. Ashcroft, and R. J. Hemley, *Proc. Natl. Acad. Sci. U.S.A.* **114**, 6990 (2017).
- [28] K. Tanaka, J. S. Tse, and H. Liu, *Phys. Rev. B* **96**, 100502 (2017).
- [29] X. Ye, N. Zarifi, E. Zurek, R. Hoffmann, and N. W. Ashcroft, *J. Phys. Chem. C* **122**, 6298 (2018).
- [30] W. Cui, T. Bi, J. Shi, Y. Li, H. Liu, E. Zurek, and R. J. Hemley, *Phys. Rev. B* **101**, 134504 (2020).
- [31] Y. Sun, Y. Tian, B. Jiang, X. Li, H. Li, T. Iitaka, X. Zhong, and Y. Xie, *Phys. Rev. B* **101**, 174102 (2020).
- [32] M. Somayazulu, M. Ahart, A. K. Mishra, Z. M. Geballe, M. Baldini, Y. Meng, V. V. Struzhkin, and R. J. Hemley, *Phys. Rev. Lett.* **122**, 027001 (2019).
- [33] A. P. Drozdov, P. P. Kong, V. S. Minkov, S. P. Besedin, M. A. Kuzovnikov, S. Mozaffari, L. Balicas, F. F. Balakirev, D. E. Graf, V. B. Prakapenka, E. Greenberg, D. A. Knyazev, M. Tkacz, and M. I. Eremets, *Nature* **569**, 528 (2019).
- [34] F. Hong, L. X. Yang, P. F. Shan, P. T. Yang, Z. Y. Liu, J. P. Sun, Y. Y. Yin, X. H. Yu, J. G. Cheng, Z. X. Zhao, *Chin. Phys. Lett.* **37**, 107401 (2020).
- [35] E. Snider, N. Dasenbrock-Gammon, R. McBride, M. Debessai, H. Vindana, K. Vencatasamy, K. V. Lawler, A. Salamat, and R. P. Dias, *Nature* **586**, 373 (2020).
- [36] A. F. Goncharov, S. S. Lobanov, I. Kruglov, X.-M. Zhao, X.-J. Chen, A. R. Oganov, Z. Konôpková, and V. B. Prakapenka, *Phys. Rev. B* **93**, 174105 (2016).
- [37] R. Akashi, W. Sano, R. Arita, and S. Tsuneyuki, *Phys. Rev. Lett.* **117**, 075503 (2016).
- [38] A. Majumdar, J. S. Tse, and Y. Yao, *Angew. Chem. Int. Ed.* **56**, 11390 (2017).
- [39] A. F. Goncharov, S. S. Lobanov, V. B. Prakapenka, and E. Greenberg, *Phys. Rev. B* **95**, 140101 (2017).
- [40] D. Laniel, B. Winkler, E. Bykova, T. Fedotenko, S. Chariton, V. Milman, M. Bykov, V. Prakapenka, L. Dubrovinsky, and N. Dubrovinskaia, *Phys. Rev. B* **102**, 134109 (2020).
- [41] X. Gonze, *Phys. Rev. B* **55**, 10337 (1997).
- [42] X. Gonze, and C. Lee, *Phys. Rev. B* **55**, 10355 (1997).
- [43] X. Gonze, G.-M. Rignanese, M. Verstraete, J.-M. Beuken, Y. Pouillon, R. Caracas, F. Jollet, M. Torrent, G. Zerah, M. Mikami, P. Ghosez, M. Veithen, J.-Y. Raty, V. Olevano, F. Bruneval, L. Reining, R. Godby, G. Onida, D. R. Hamann, and D. C. Allan, *Z. Kristallogr.* **220**, 558 (2005).
- [44] X. Gonze, B. Amadon, P.-M. Anglade, J.-M. Beuken, F. Bottin, P. Boulanger, F. Bruneval, D. Caliste, R. Caracas, M. Côté, T. Deutsch, L. Genovese, Ph. Ghosez, M. Giantomassi, S. Goedecker, D. R. Hamann, P. Hermet, F. Jollet, G. Jomard, S. Leroux, M. Mancini, S. Mazevet, M. J. T. Oliveira, G. Onida, Y. Pouillon, T. Rangel, G.-M. Rignanese, D. Sangalli, R. Shaltaf, M. Torrent, M. J. Verstraete, G. Zerah, and J. W. Zwanziger, *Comput. Phys. Commun.* **180**, 2582 (2009).
- [45] C. Hartwigsen, S. Goedecker, and J. Hutter, *Phys. Rev. B* **58**, 3641 (1998).
- [46] S. Baroni, S. D. Gironcoli, A. D. Corso, and P. Giannozzi, *Rev. Mod. Phys.* **73**, 515 (2001).
- [47] P. B. Allen, and B. Mitrović, *Solid State Physics* **37**, 1 (1983).
- [48] P. B. Allen, and R. C. Dynes, *Phys. Rev. B* **12**, 905 (1975).
- [49] A. P. Durajski, R. Szcześniak, and Y. Li, *Physica C* **515**, 1 (2015).
- [50] *The Electron-Phonon Interaction in Metals*, Selected Topics in Solid State Physics Vol. 16, edited by E. P. Wohlfahrt (North-Holland, Amsterdam, 1981).
- [51] P. B. Allen and M. L. Cohen, *Phys. Rev. Lett.* **29**, 1593 (1972).
- [52] Y. Quan, S. S. Ghosh, and W. E. Pickett, *Phys. Rev. B* **100**, 184505 (2019).
- [53] X.-J. Chen, *Matter Radiat. Extremes* **5**, 068102 (2020).